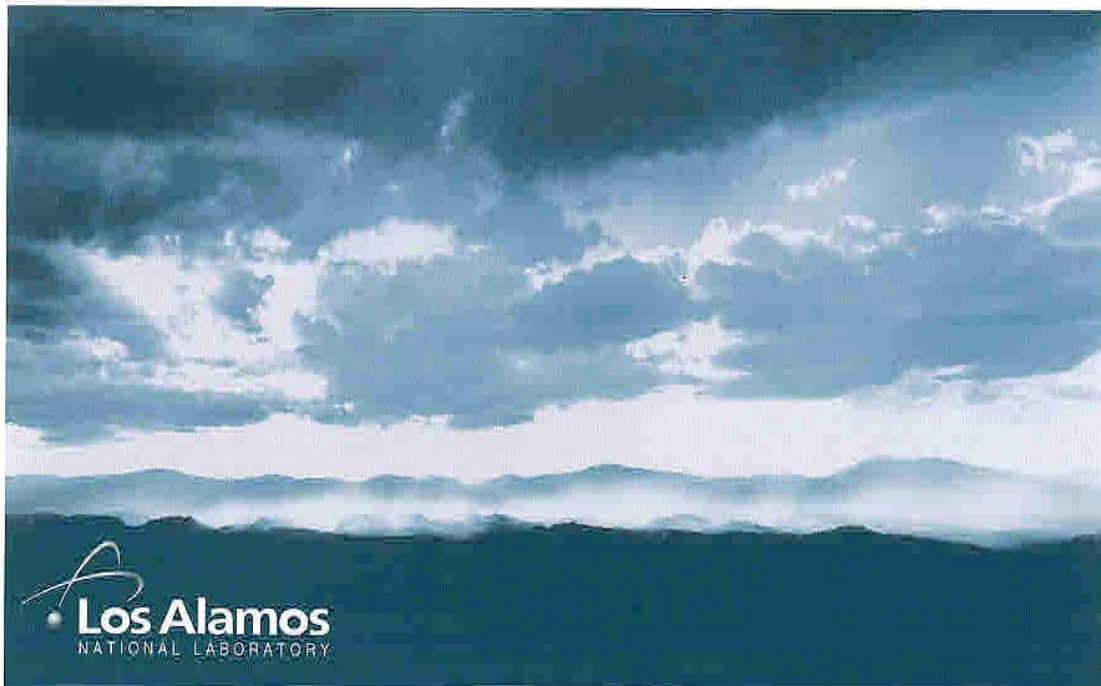


Large-Area Neutron Detector based on Li-6 Pulse Mode Ionization Chamber

K. Chung, K. Ianakiev, M. Swinhoe, and M. Makela
Los Alamos National Laboratory
Los Alamos, New Mexico, USA

*Presented at the
Institute of Nuclear Material Management
46th Annual Meeting
Phoenix, Arizona
July 10-14, 2005*



Chris J. Lindberg

Large-Area Neutron Detector based on Li-6 Pulse Mode Ionization Chamber

K. Chung, K. Ianakiev, M. Swinhoe, and M. Makela
Los Alamos National Laboratory
Los Alamos, New Mexico, USA

Abstract

Prototypes of a Li-6 Pulse Mode Ionization Chamber (LiPMIC) have been in development for the past two years for the purpose of providing large-area neutron detector. This system would be suitable for remote deployment for homeland security and counterterrorism needs at borders, ports, and nuclear facilities. A prototype of LiPMIC is expected to provide a similar level of performance to the current industry-standard, He-3 proportional counters, while keeping the initial cost of procurement down by an order of magnitude, especially where large numbers of detectors are required.

The overall design aspect and the efficiency optimization process will be discussed. Specifically, the MCNP simulations of a single-cell prototype were performed and benchmarked with the experimental results. MCNP simulations of a three dimensional array design show intrinsic efficiency comparable to that of an array of He-3 proportional counters. LiPMIC has shown steady progress toward fulfilling the design expectations and future design modification and optimization are discussed.

Introduction

We are developing a unique ${}^6\text{Li}$ neutron-capture pulse mode ion chamber (LiPMIC) for neutron detection. The motivation is to produce a detector that is suitable for mass production and large-scale deployment needed for homeland security and counter terrorism applications. This novel pulse-mode ion chamber is specifically designed as one of more cost-effective instruments [1] that have the potential to fulfill the homeland security and counter-terrorism as well as material control and accountability needs for large-scale deployment in a distributed network of long-term remote sensors. For those needs, the detector is expected to provide non-invasive interrogation of goods and personnel at borders, ports, strategic landmarks, and buildings for detecting nuclear materials such as plutonium. The LiPMIC is expected to provide neutron detection capability for such deployment at comparable performance levels to the currently available neutron detectors while reducing the procurement cost by an order of magnitude [1]. The purpose of this report is 1) to address the progress in designing and optimizing the performance of this detector that can overcome the fill-gas contamination stemming from outgas of detector parts and 2) to provide a demonstration of performance for prototypical LiPMICs.

General Characteristics and Detection Mechanism

Figure 1 is a diagram of a single cell prototype. The high-density polyethylene (HDPE) body is made from two machined parts and serves multiple purposes as a neutron moderator, electrical insulator, and physical shell. Ion chambers traditionally detect radiation by collecting ion-electron pairs produced from the interactions between radiation and fill-gas atoms. In the LiPMIC incident neutrons are thermalized in the HDPE and interact with ${}^6\text{Li}$ atoms in the Li metal (green line) applied on a metal substrate surface (red line), which also acts as cathode, and produces the primary charged particles from the interactions. The resultant primary charged particles, tritons and alpha particles, interact with argon gas atoms and produce electrons and argon ions, which are the electronic signal carriers. The inside dimension of the active volume of the single cell prototype in Figure 1 is 5"x 5" and 2.5" (height). The height was chosen with the range of a triton in 1 ATM of argon gas. The metal substrate is applied onto the bare HDPE walls by proven technologies such as physical vacuum deposition and is less than 50 μm thick. The two HDPE pieces are bolted together with a gasket in between to seal the interface. The

chamber also houses two gas pipes so that the gas can be changed for measurement with different fill-gas combination.

Figure 2 provides views from top and cut-away section of a matrix design. The HDPE thickness at different locations in the matrix is determined by optimization for maximum reaction rate at ${}^6\text{Li}$ inside the volume. A matrix design is a logical progress from a single cell design. Having multiple cells will increase the probability of catching the neutrons that escape the single cell and will increase the overall efficiency.

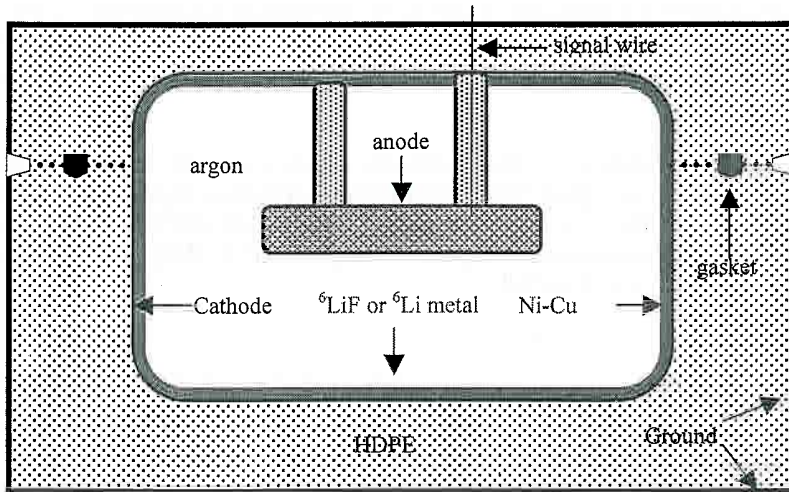


Figure 1 Conceptual design of a single cell prototype.

In $\text{He}3$ proportional counters neutrons interact in the entire gas volume whereas the interactions between thermal neutrons and ${}^6\text{Li}$ occur in the thin ${}^6\text{Li}$ layer for LiPMIC. In LiPMIC an incident neutron collides with a stationary ${}^6\text{Li}$ atom. The nucleus is fragmented into a triton and an alpha particle, emitted with back-to-back symmetry at 180 degrees (when incident neutron is sufficiently slow enough) with 2.7 and 2.1 MeV, respectively, as shown in Table 1 [2]. The back-to-back symmetry limits the overall probability of detection for the resultant particles because one will almost always be attenuated within the ${}^6\text{Li}$ whereas in $\text{He}3$ detector the two resultant particles are borne in the gas volume, and both particles deposit their energy in the gas.

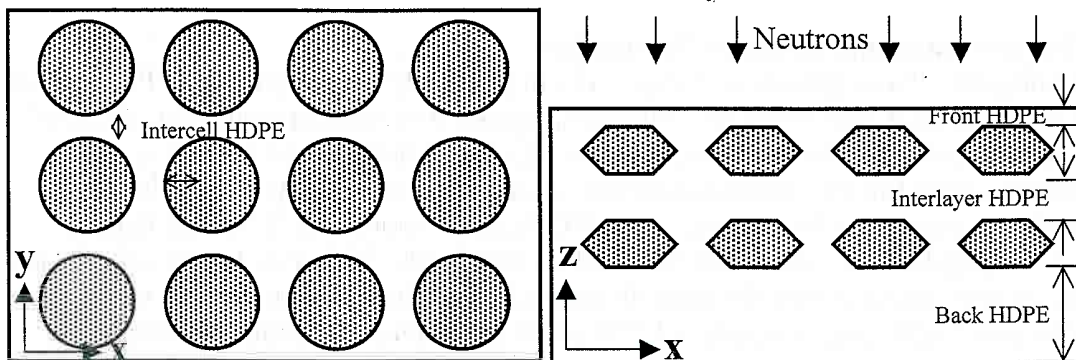


Figure 2 View from top and cut-away view from the side for a cell matrix prototype.

To consider the probability of interaction for a detector as a whole, a quick calculation of total cross section can be performed. The total cross section can be thought of as the collective cross section the detector presents to an incident neutron. The total cross section is the product of

macroscopic cross section and volume of the interaction site. The similar total cross section values shown in Table 1 between He3 detector and LiPMIC indicate that two detectors are not much different from each other in the theoretical limit of interaction probability when a thermal neutron reaches the interaction site. The calculation of total cross section is a little different for He3 detector where the total number of He atoms is derived from the effective volume of the He gas at 4 ATM inside the tube. Total cross section for LiPMIC is derived as the following:

$$\begin{aligned} (\text{Areal Density}) * (\text{Surface Area}) &= \text{Total Mass} \\ \left(\frac{\text{Total Mass}}{\text{Mole Mass}}\right) * N_A &= \text{Number of Atoms} \\ (\text{Number of Atoms}) * \left(\frac{\text{Cross Section}}{\text{Atom}}\right) &= \text{Total Cross Section } [\text{cm}^2] \end{aligned}$$

The relationship between total cross section and macroscopic cross section can be established with the following derivation:

$$\begin{aligned} \text{Total Cross Section} &= (\rho * x * A) * \frac{N_A}{M_w} * \sigma \\ &= \rho * \frac{N_A}{M_w} * xA * \sigma = N * V * \sigma \\ &= N * \sigma * V = \Sigma_t V \end{aligned}$$

Table 1 Comparison between HeGPC and LiPMIC.

	³ He Prop. Counter	⁶ Li neutron-capture pulse mode ion chambers (LiPMIC)
Interaction Site	³ He Gas @ 4 ATM @ 30 cm	⁶ Li metal @ 30μm
Interaction mode	³ He(n,p) ³ H	⁶ Li(n,t) ⁴ He
Q-value	0.765 MeV	4.8 (t:2.7; α:2.1 MeV)
Thermal neutron cross section	5330 barns	940 barns
Active Area/Vol.	150 cm ³	~800 cm ²
Cost	~\$1200/tube	< \$200/cell [1]
Areal density	0.54 mg/cm ² (thickness=r)	1.38 mg/cm ²
Total reaction cross section	86 cm ²	63* cm ²

*Effective total reaction cross section=total reaction cross section x escape probability (60% @ 30 um of ⁶Li)

Neutron Simulation Using MCNPX

MCNPX is an industry-standard tool in simulating neutron interaction [3]. Because one of the particle interaction modes of interest is slowing down and capturing of source neutrons in the moderator and subsequently in ⁶Li, MCNPX is one of the best simulation tools for the purpose of obtaining information on the behavior of the neutrons in the HDPE and ⁶Li. MCNPX is also used to calculate the optimal thickness of ⁶Li for both interaction and escape probability of the primary charged particles. As the ⁶Li layer gets thicker, a smaller fraction of the resultant particles will escape the metal. On the other hand, if the ⁶Li is too thin there will be fewer primary charged particles produced. Figure 3 shows that the reaction rate per orthogonally incident neutron reaches almost 30% at 100 μm thickness, but less than 10% of the primary charged particles get out of the ⁶Li, reducing the efficiency to less than 10%. At 30 μm one-third less number of primary charged particles are produced, but also fewer of them are attenuated in the ⁶Li and has better efficiency than at 100 μm.

Having obtained the optimal thickness of ${}^6\text{Li}$, one can proceed with the MCNPX simulation for HDPE thickness design. MCNPX is used for neutron interaction simulation in the HDPE to obtain the optimal thickness for source neutron to thermal neutron energy transition. The simulations are fundamental in optimizing the ion chamber's performance as the design attempts to collect neutrons as efficiently as possible in the form of thermal neutrons within practical constraints imposed by size limitation, power consumption, etc.

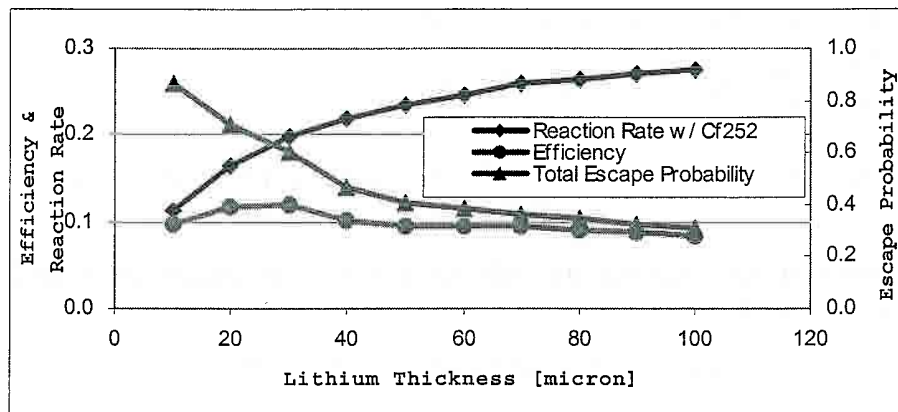


Figure 3 Optimizing lithium thickness for both reaction and escape probability.

Figure 4 is a summary of HDPE thickness optimization simulations for metal chambers. This is another series of prototypes that are being considered in parallel with plastic chambers with HDPE body. For the optimization, individual pieces of HDPE's are defined as front, interlayer, and back HDPE with respect to the position of the center of an ion chamber. The front HDPE is the block of HDPE the source neutrons have to penetrate before they reach the ion chambers. Figure 2 is a graphical depiction of the location of the various HDPE's. Because the matrix contains 2 layers of detection chambers, there exists an interlayer of HDPE, which provides some backscattering to the first row of chambers and more moderation to the second row. The intercell spacing for this prototype was set constant for this series of simulations. The back HDPE is the block of HDPE located behind the second layer of ion chambers.

Plots in Figure 4 can be divided into three groups. The MCNPX simulation sought to ascertain the optimal HDPE thickness in a metal chamber matrix shown in Fig. 2 (2 layers of 3x4 cells). The optimization process can be thought of as finding a function that defines the maximum interaction rate in multi-variable space made up of front, interlayer, back HDPE thickness. The combination of thickness for the 3 areas was investigated by trial and error. By keeping the other two variables constant while varying the other, the effect of change by the variable was recorded. The first group is the back HDPE thickness variation plots (diamond data points). The thickness of back HDPE was varied to obtain the thickness that produces the highest efficiency within the localized space of back HDPE thickness variable. When the back HDPE thickness reaches 10 cm, adding more HDPE did not improve the efficiency.

Further series of simulations for the interlayer thickness were not performed because they were integrated into the other two series with front and back thickness variation. The interlayer thickness of 3.81 cm (1.5") produces a high efficiency and has the best efficiency to thickness ratio. The simulations with front thickness of HDPE variation (square data points) more or less follow the prediction of exponentially decreasing interaction probability as a function of thickness.

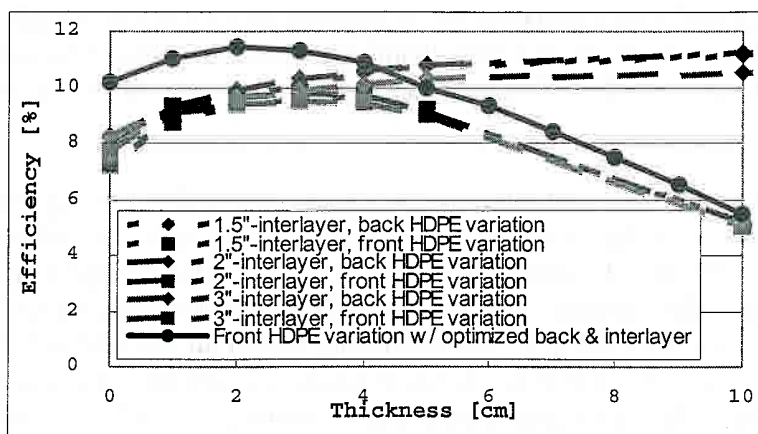


Figure 4 Optimizing the HDPE thickness in metal tray chamber matrix.

Another series of simulations was performed by varying the front thickness from 0 to 10 cm while keeping the interlayer and back thickness optimized at 4 cm and 7.5 cm, respectively. The solid black line with circular data points shows the total efficiency from this series. The best efficiency of 11.5% from a preliminary series of simulations is puzzling because there are many instances in the simulation where the efficiency is less than 1% smaller than the best efficiency. This will be investigated in the future, as the surface area of ${}^6\text{Li}$ will be varied for comparison. By varying the surface area, it will be determined if the attenuation of primary charged particles in ${}^6\text{Li}$ is the inherent limiting factor, or if the systematic limitation such as converting fast neutrons to thermal neutrons is the cause.

Incorporation of Outgas and Garfield Simulation

One of the premises for stable operation of gaseous detectors in general is that the content of the fill-gas does not change throughout the intended lifetime. This is particularly true for most proportional counters whose gas multiplication feature is a great advantage, but also could be an Achilles' heel for sealed gas designs because it relies on unchanging fill-gas. It was realized from early on in this research that the use of HDPE and the infeasibility of purification mechanisms during the proposed deployment would not allow most gas proportional counter designs. Not operating in the gas multiplication region is usually a disadvantage because the signal size is reduced; however, in this case, it allows long-term, stable operation of the ion chamber even with accumulating outgas because working in lower voltage prevents photopolymerization from gas multiplication and deposits forming on the anode wires, which are classical aging effects [4]. In addition, avoiding gas multiplication reduces the sensitivity to gas composition. While this operational condition removes the classical aging effects, the detector design has to deal with the outgas from the detector parts.

To test how much an ion chamber body made out of metallized HDPE would outgas in a short period, a metallized HDPE single-cell chamber was put under negative pressure for 4 months, starting with an initial pressure of 0.9 millitorr under vacuum. The chamber was locked down, and pressure was checked with a residual gas analyzer at the end of first month and fourth month. During this period, the accumulated pressure inside the detector was 1.7 and 2.6 torr, respectively [5]. If this rate of 0.3 torr/month between second and fourth month is assumed conservatively to continue during the lifetime of the ion chamber, after 20 years of continuous service the detector would accumulate 73 torr of outgas, which would amount to approximately 10% of the atmospheric pressure. Although a preliminary observation identified environmental gas such as nitrogen and oxygen as the major constituents, a more precise measurement setup for outgas is needed to identify the content. There is some amount of light hydrocarbon gas present

in the outgas and the Garfield [6] simulation focused on the accumulation of light hydrocarbon gas in the detector volume. Garfield is a drift chamber simulation package for gas transport in electrostatic fields, developed at CERN, which has been used to investigate the expected result of outgas in the detector.

Figure 5 is a summary of electron drift velocity calculated with Garfield in argon-methane gas mixtures. After the interaction has occurred in the ${}^6\text{Li}$ and the primary charged particles are ejected into the fill-gas mixture, the interactions between either triton or alpha particle and fill gas atoms are simulated with Garfield. The accuracy of Garfield has been verified with gas transport data accumulated at CERN [7]. The interesting feature in this plot is the convergence of electron drift velocity of 3.5 cm/ μsec for different methane concentration at reduced electric field intensity of 0.06 to 0.09 V/cm*Torr, which is equivalent to 170 to 260 volts of high voltage bias. The electron drift velocity between 4% and 15% of methane concentration remains fairly constant in the said field strength range. This indicates that the electron drift velocity will be affected minimally by the accumulation of methane in the fill-gas. The significance of this finding is that an ion chamber, when properly designed, can operate with additional accumulation of hydrocarbon in the fill-gas. An argon-isobutane mixture exhibited similar behavior near 0.5 V/cm*torr between 5% and 20% concentration of isobutene. Knowing the outgassing content and rate, the ion chamber can be designed so that the appropriate drift velocity is maintained under specified electric field strength. Similar simulations are planned with the actual outgas content to extend the results to a more applicable deployment condition.

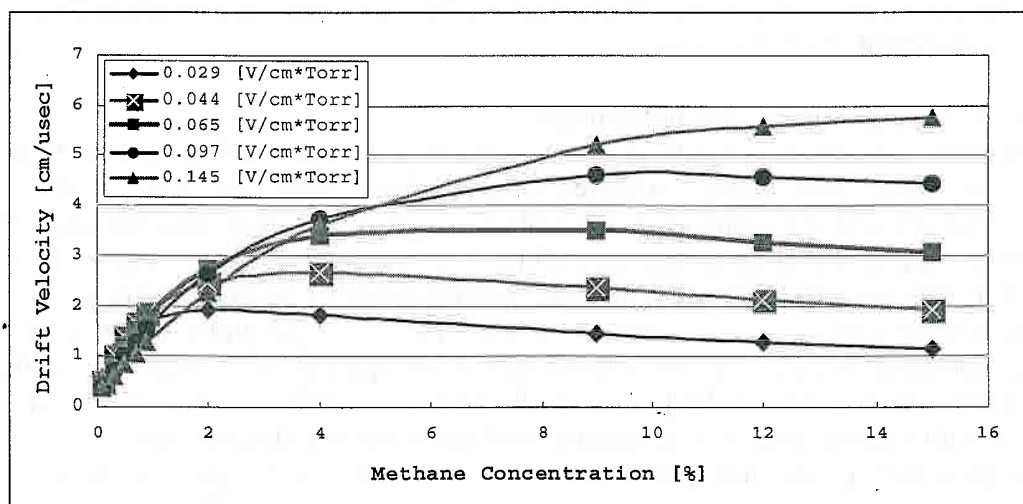


Figure 5 Drift velocity of electrons in Ar-CH₄ gas mixtures as a function of field strength.

Experiments

Having obtained from the Garfield simulation the target electron velocity, measurements were performed with various methane concentrations and with different shaping times. Fig. 6 is a comparison measurement of three Cs-137 gamma sources and Cf-252 neutron source. The activity of the Cs-137 sources was reported as 0.96 mCi and the Cf-252 source strength was calculated as 0.03 mCi. The gamma activity is below 2 fC and when a region of interest for neutron counting is setup for 90%, then the lower energy threshold will effectively remove contribution from gamma sources, which are single pulses and not pileups.

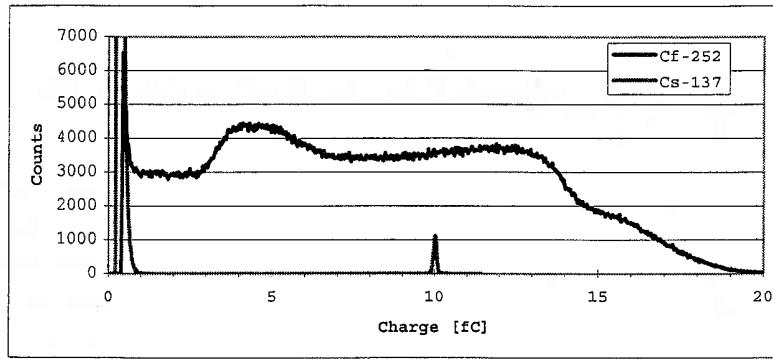


Figure 6 Gamma sensitivity of a LiF single cell prototype.

Figure 7 is the comparison of normalized total counts at different methane concentrations when the signal is collected with 2 μ sec shaping time. The Garfield simulation predicted that at above 4% of methane concentration and above 170V, the electron velocity would be stabilized. Fig. 7 supports this finding with the total counts maintaining above 95% for all 5, 7.5, and 10% methane concentration and also above 200V with an exception of 2.5% methane concentration plot.

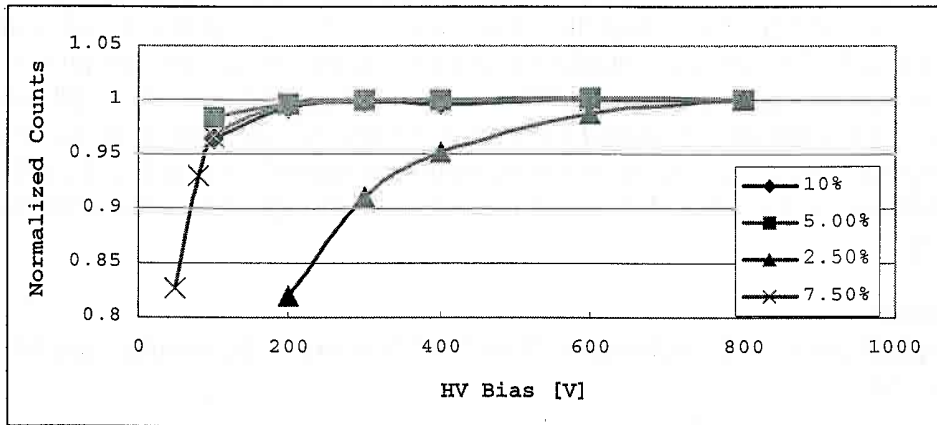


Figure 7 Normalized total counts at 2 microsecond shaping time.

In order to choose the appropriate shaping time for 10% methane fill-gas, Fig. 8 shows that a shaping constant of 2 μ Sec or longer is adequate for collecting pulses. Choosing as short a shaping time as possible can reduce the sensitivity to microphonics because shorter shaping time periods are likely to reduce the effect of the real pulses piling on long microphonic noise pulses. One potential method of increasing the efficiency of the detector is to increase the surface area of the deposit by covering the anode as well as the cathode with a Li layer. In order to quantify the gain to be made, the anode alone was painted with ^6LiF and the spectrum was observed. The spectrum from cathode surface registered 3700 cps while the spectrum from painted anode registered 700 cps. The ratio between the total counts corresponded to the ratio between the surface areas of the two. Thus, coating the anode will give a proportional increase in efficiency. Further measurements with variation of gas mixtures are necessary to maximize the gain.

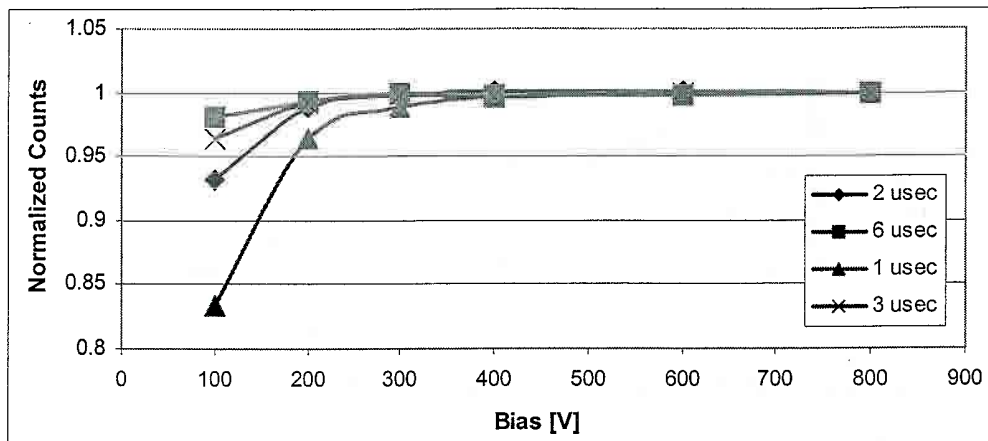


Figure 8 Normalized total counts at 10% methane concentration.

Conclusion

The LiPMIC is a novel, gaseous detector that is designed to serve large scale, remote deployment of neutron detectors. The LiPMIC is optimized for moderation of the incident neutrons to thermal energy and for the creation of primary charged particles in the fill-gas. It is believed that the final design of the LiPMIC will match the performance of He-3 gas proportional counters. Simulations performed with Garfield have shown that certain mixtures of fill-gas allow stable electron drift velocity through a surprisingly wide range of concentrations. The exact content and rate of outgas still needs further quantification, but the preliminary measurements with the single cell prototypes were performed to obtain the basic operational parameters. Future series of prototypes will be used for detailed measurements of verifying operational parameters and of accelerated aging test.

Acknowledgements

This work is funded by the US Department of Homeland Security under contract number HSSCHQ-04-X-00387.

Reference

- [1] K.Ianakiev, M.Swinhoe "An Affordable Large Area Neutron Detector Suitable for Mass Production" Final Report for LDRD project 20020342ER.
- [2] G.Knoll, Radiation Detection and Measurement, John Wiley & Sons, Inc., 2000.
- [3] J.S.Hendricks and G.W.McKinney, MCNPX v2.4.e, Los Alamos National Lab, 2002.
- [4] M.Titov, "Radiation Damage and Long-Term Aging in Gas Detectors," Presented at INFN ELOISATRON 2003.
- [5] K. Ianakiev, M.T.Swinhoe, K.Chung and E.A.McKigney, "Large Area Neutron Detector Based on ⁶Li Ionization Chamber with Integrated Body-Moderator of High Density Polyethylene," Presented at IEEE 2004.
- [6] R.Veenhof, GARFIELD, CERN, 1984.
- [7] A.Peisert and F.Sauli, Drift and Diffusion of Electrons in Gases, CERN 84-08, 1984.